

# Preparation of $\text{Li}_4\text{Ti}_5\text{O}_{12}$ spherical particles for rechargeable lithium batteries<sup>☆</sup>

Kiyoshi Kanamura<sup>a,b,\*</sup>, Takeshi Chiba<sup>a,b</sup>, Kaoru Dokko<sup>a,b</sup>

<sup>a</sup> Department of Applied Chemistry, Graduate School of Engineering, Tokyo Metropolitan University, 1-1 Minami-ohasawa, Hachioji, Tokyo 192-0397, Japan

<sup>b</sup> CREST, Japan Science and Technology Agency, Kawaguchi, Saitama 332-0012, Japan

Available online 1 August 2005

## Abstract

Spherical  $\text{Li}_4\text{Ti}_5\text{O}_{12}$  particles were prepared via an emulsion-gel process. The preparation of spherical  $\text{Li}_4\text{Ti}_5\text{O}_{12}$  such as the concentrations of the starting materials and heat treatment were optimized. The particle size distribution of the  $\text{Li}_4\text{Ti}_5\text{O}_{12}$  prepared under optimized condition was very narrow, and the particle size was 0.45  $\mu\text{m}$ . It was found that a short heat treatment in an infrared furnace was useful to crystallize amorphous Li–Ti–O powders without aggregation of particles or morphology change. The obtained  $\text{Li}_4\text{Ti}_5\text{O}_{12}$  had the spinel structure, and was phase pure. The prepared  $\text{Li}_4\text{Ti}_5\text{O}_{12}$  exhibited a high discharge capacity of 160 mA h  $\text{g}^{-1}$  at the potential of 1.5 V versus  $\text{Li}/\text{Li}^+$ , and the charge–discharge cycle stability was excellent.

© 2005 Elsevier Ltd. All rights reserved.

**Keywords:** Batteries; Sol–gel processes; Spinel;  $\text{Li}_4\text{Ti}_5\text{O}_{12}$

## 1. Introduction

Rechargeable lithium-ion battery using liquid electrolytes suffers from several safety concerns.<sup>1</sup> The most significant problem is its flammability.<sup>2,3</sup> In order to solve safety problem of rechargeable lithium-ion batteries, solid electrolytes have been studied to construct all solid-state rechargeable lithium battery that exhibit no flammability. However, several problems still remain to realize all solid-state battery, such as low conductivity of solid electrolytes,<sup>4</sup> and high contact resistance between electrode materials and solid electrolyte. A volume change of electrode materials during charge and discharge produces an internal strain in electrodes, which will be a factor of battery failure. Then, electrode materials, which do not show serious volume change, should be selected for all solid-state batteries. It is well known that spinel-related  $\text{LiMn}_2\text{O}_4$ <sup>5</sup> and  $\text{Li}_4\text{Ti}_5\text{O}_{12}$  show a very small volume change during charge and discharge,<sup>6–15</sup> and they are promising candidates for cathode and anode of all solid-state rechargeable lithium batteries, respectively.

In this study, spherical  $\text{Li}_4\text{Ti}_5\text{O}_{12}$  particles were prepared using an emulsion-gel process. The emulsion-gel process is a derivative of sol–gel method.<sup>16–19</sup> The gelation process proceeds in a water–oil emulsion. A micro-droplet in the emulsion is utilized as micro-reactor, so that both hydrolysis and condensation of metal alkoxides take place in the droplet, and spherical particles of amorphous metal oxides can be prepared. The amorphous particles can be crystallized at relatively low temperature, and chemical composition of the obtained ceramic is homogeneous compared to one prepared by standard solid-state synthesis. This is the first report on novel synthesis of  $\text{Li}_4\text{Ti}_5\text{O}_{12}$  by emulsion-gel process with heat treatment. The conditions to prepare spherical  $\text{Li}_4\text{Ti}_5\text{O}_{12}$  with narrow size distribution were optimized, and the electrochemical properties of the prepared  $\text{Li}_4\text{Ti}_5\text{O}_{12}$  were characterized.

## 2. Experimental

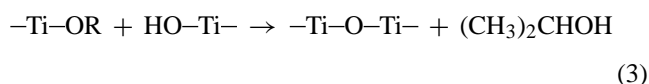
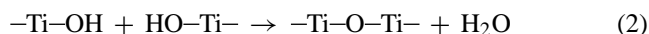
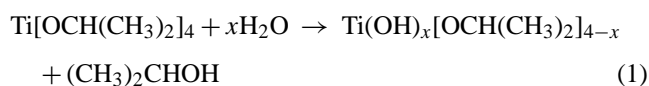
Titanium tetraisopropoxide (TTIP) was mixed with 180 mL of *n*-octanol and 0.3 g of hydroxypropyl cellulose (HPC, Mw = 62,500). The solution was stirred with an emul-

<sup>☆</sup> This paper was presented at ISiem2004, Paper Number 167.

\* Corresponding author. Tel.: +81 426 77 2828; fax: +81 426 77 2828.

E-mail address: [kanamura-kiyoshi@c.metro-u.ac.jp](mailto:kanamura-kiyoshi@c.metro-u.ac.jp) (K. Kanamura).

sifier (DIAX900, Heidolph) at 40 °C for 15 min. Subsequently, 120 mL of acetonitrile was added into the solution, and it was stirred for 30 min. At this stage, emulsion was generated, and TTIP dissolved into acetonitrile droplets. The hydroxypropyl cellulose stabilized the emulsion. The concentration of TTIP in the total solution was controlled to be 0.02–0.12 mol dm<sup>-3</sup>. Then, 7.2 mL of lithium hydroxide aqueous solution was poured into the mixed solution, and it was stirred for 60 min. Excess LiOH was put into the solution, and the molar ratio of Li:Ti was controlled to be 1:1. The excess LiOH was effective in preventing the generation of impurities such as TiO<sub>2</sub>. Water could not dissolve into octanol but acetonitrile, so that the hydrolysis of TTIP described by Eq. (1) and condensation according to Eqs. (2) and (3), took place in the acetonitrile droplets during the last stirring process.



Furthermore, Li<sup>+</sup> was also inserted in the particles, and amorphous Li–Ti–O spherical particles were generated. In this way, the droplet of acetonitrile was used as a micro-reactor. This is a characteristic of emulsion-gel process. The Li–Ti–O particles were separated from the solution by centrifugation, and the precipitate was washed with ethanol to eliminate the organic solvents and residual LiOH. The obtained powder was dried with freeze dryer (FDU-810, EYELA). Then, the obtained amorphous Li–Ti–O was calcinated at 500 °C for 3 h. Further heat-treatments were carried out with an electric furnace (SUPER-BURN, Motoyama) or an infrared furnace (VHT-E44, Ulvac) at 800 °C in air. The prepared samples were characterized with X-ray diffraction (RINT-2000, Rigaku) and scanning electron microscope (JSM-5310, JEOL).

A beaker-type electrochemical cell was fabricated for charge–discharge tests. To make the working electrode, 70 wt% sample, 15 wt% Ketjen black, and 15 wt% polyvinylidene fluoride were mixed together in *N*-methylpyrrolidinone. The prepared slurry was spread uniformly on a thin aluminum foil, and it was dried overnight at 100 °C in vacuum. The area of the working electrode was 1.5 cm<sup>2</sup>. A lithium foil was used as the counter electrode, and a porous polypropylene film was used as a separator. All electrochemical measurements were performed with two-electrode system. A mixed solvent of ethylene carbonate (EC) and diethyl carbonate (DEC) (1:1 in volume) containing 1.0 mol dm<sup>-3</sup> LiClO<sub>4</sub> was used as an electrolyte. Galvanostatic charge–discharge test was performed using automatic charge–discharge equipment

(HJR-110mSM6, Hokuto Denko Co.) in a potential range of 3.0–1.2 V at 0.1 C rate (16.7 mA g<sup>-1</sup>). All electrochemical experiments were conducted in an argon-filled glove box at room temperature.

### 3. Results and discussion

Fig. 1 shows the scanning electron microphotographs (SEM) of amorphous Li–Ti–O prepared by the emulsion-gel method. The spherical particles were obtained, and the size of prepared particle was 0.3–1.0 μm in diameter. The particle size distribution changed depending on the concentration of TTIP. In the cases of the low concentration of TTIP (0.02–0.04 mol dm<sup>-3</sup>), the particle size was about 0.45 μm with narrow size distribution. However, as increasing TTIP concentration, the particle size distribution became broader, and the larger particles, ca. 1 μm, also appeared. *iso*-Propanol was released during the hydrolysis step. It was considered that the amount of *iso*-propanol affected the stabilization of emulsion. If the amount of *iso*-propanol is large, the emulsion is destabilized and the aggregation of droplets takes place.<sup>18</sup> In the present study, the concentration of TTIP should be lower than 0.05 mol dm<sup>-3</sup> to obtain the particles with narrow size distribution, and TTIP was set to be 0.03 mol dm<sup>-3</sup> to prepare Li–Ti–O particles in the following experiments.

The amorphous Li–Ti–O synthesized by the emulsion method showed no XRD peaks as displayed in Fig. 2(a). The XRD pattern of the sample calcinated at 500 °C showed several peaks (Fig. 2(b)), although the peaks are broad and the sample is not so highly crystallized. The calcinated powder was further heat-treated with an electric furnace or an infrared furnace. Fig. 2(c) shows the XRD pattern of the Li<sub>4</sub>Ti<sub>5</sub>O<sub>12</sub> heat-treated with electric furnace at 800 °C for 10 h. The peaks became very sharp, and it was suggested that the sample was well crystallized by the heat-treatment. This XRD pattern showed good agreement to that reported in the literature.<sup>7</sup> Any other phases such as rutile or anatase TiO<sub>2</sub>, which were the most possible impurities, were not detected. In the case of heat treatment with infrared furnace, the temperature was elevated rapidly at 800 °C min<sup>-1</sup> and kept at 800 °C for 1 min, and then reduced quickly to 300 °C. The temperature of the sample was monitored with a thermo-couple. Fig. 2(d) shows the XRD pattern of the Li<sub>4</sub>Ti<sub>5</sub>O<sub>12</sub> heat-treated in infrared furnace, which is very similar to Fig. 2(c). This suggests that the very short heat treatment in infrared furnace is enough to crystallize the sample. Fig. 3 shows SEM images of Li<sub>4</sub>Ti<sub>5</sub>O<sub>12</sub> samples heat-treated in electric furnace and infrared furnace. The sample heat-treated in electric furnace was sintered and the aggregation of particles was observed. In the case of heat treatment with infrared furnace, serious aggregation of particles did not take place, and spherical shape of particles was maintained even after heat treatment. This is probably due to the extremely short heat treatment duration.

Fig. 4 shows the charge–discharge curves of Li<sub>4</sub>Ti<sub>5</sub>O<sub>12</sub> samples heat-treated under various conditions. All sam-

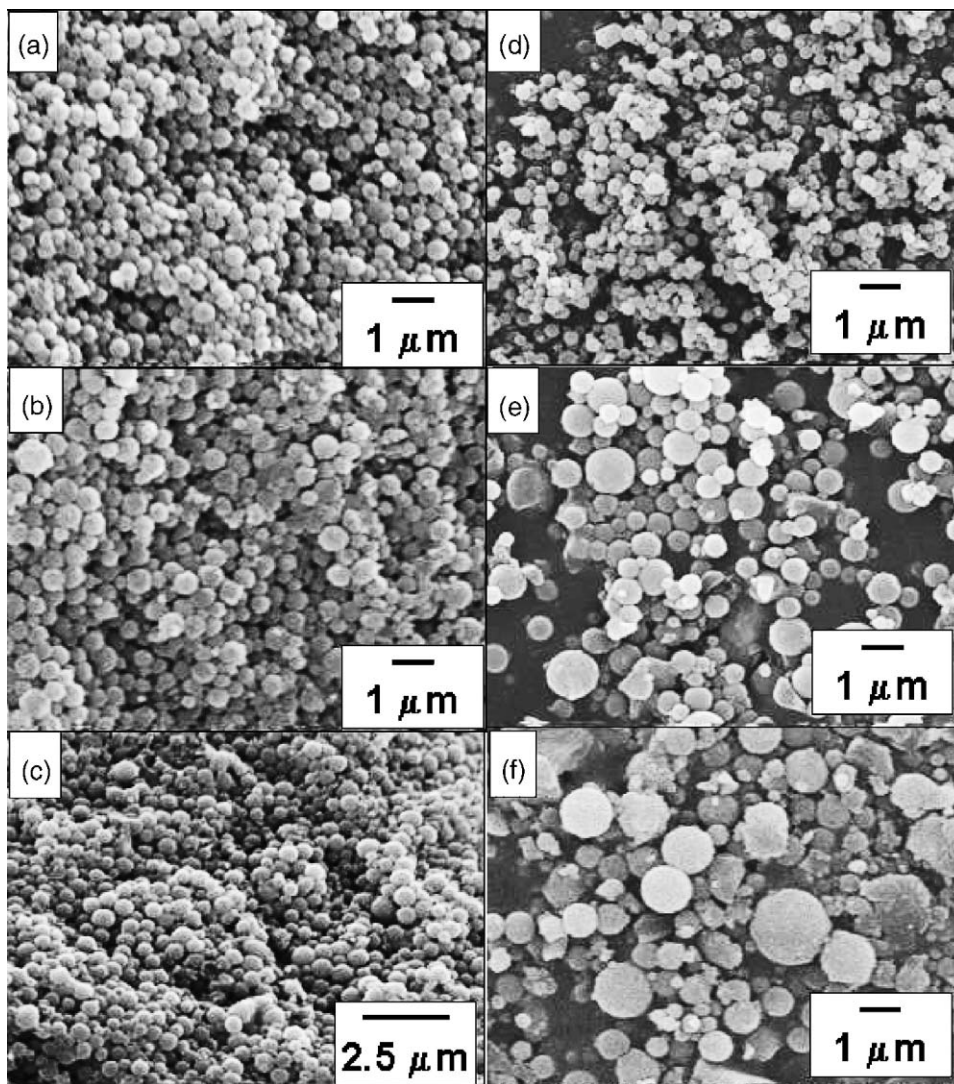


Fig. 1. SEM images of amorphous Li–Ti–O spherical particles prepared by emulsion-gel process with various concentrations of titanium tetraisopropoxide: (a) 0.02 mol dm<sup>-3</sup>; (b) 0.03 mol dm<sup>-3</sup>; (c) 0.035 mol dm<sup>-3</sup>; (d) 0.04 mol dm<sup>-3</sup>; (e) 0.08 mol dm<sup>-3</sup>; and (f) 0.12 mol dm<sup>-3</sup>.

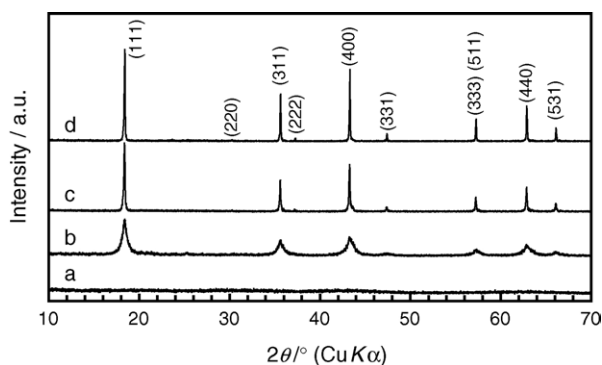
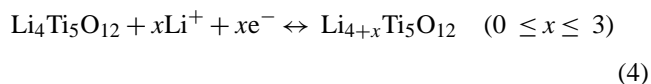


Fig. 2. Powder XRD patterns of Li–Ti–O prepared via an emulsion-gel process with various heat treatments: (a) not heat-treated; (b) calcinated at 500 °C for 3 h; (c) heat-treated at 800 °C in an electric furnace for 10 h; and (d) heat-treated at 800 °C in an infrared furnace for 1 min.

ples exhibited discharge capacity of 160 mA h g<sup>-1</sup>, which was very close to the theoretical capacity (167.5 mA h g<sup>-1</sup>). Although a small irreversible capacity was observed in the first cycle, which might be due to an irreversible electrochemical decomposition of the electrolyte, the coulombic efficiency of charge and discharge in the subsequent cycles was more than 99%. The charge and discharge mechanism of Li<sub>4</sub>Ti<sub>5</sub>O<sub>12</sub> has been discussed thoroughly in the literatures.<sup>7–11</sup> Briefly, Li<sup>+</sup> ion insertion/extraction takes place into/from crystallographic structure of Li<sub>4</sub>Ti<sub>5</sub>O<sub>12</sub> in the course of solid-state redox reaction of Ti<sup>3+/4+</sup>, as described in Eq. (4).



The shape of discharge curve of Li<sub>4</sub>Ti<sub>5</sub>O<sub>12</sub> depended on the heat treatment condition. The flat charge and discharge

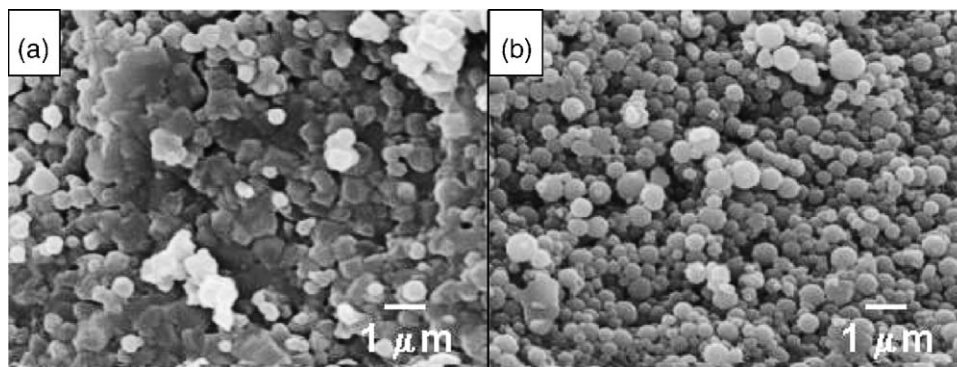


Fig. 3. SEM images of  $\text{Li}_4\text{Ti}_5\text{O}_{12}$  particles heat-treated (a) at  $800^\circ\text{C}$  in an electric furnace for 10 h, and (b) at  $800^\circ\text{C}$  in an infrared furnace for 1 min.

curves were observed at 1.55 V versus  $\text{Li}/\text{Li}^+$  for samples heat-treated at  $800^\circ\text{C}$  (Fig. 4(b) and (c)), which was an intrinsic electrochemical property of  $\text{Li}_4\text{Ti}_5\text{O}_{12}$  spinel. Fig. 4(a) shows the charge–discharge curves of  $\text{Li}_4\text{Ti}_5\text{O}_{12}$  heat-treated at  $500^\circ\text{C}$ . This sample showed a small discharge capacity in a potential range from 1.50 to 1.20 V besides the 1.55 V plateau. As can be seen in Fig. 2(b), the crystallinity of this sample was low. The discharge capacity in the potential range

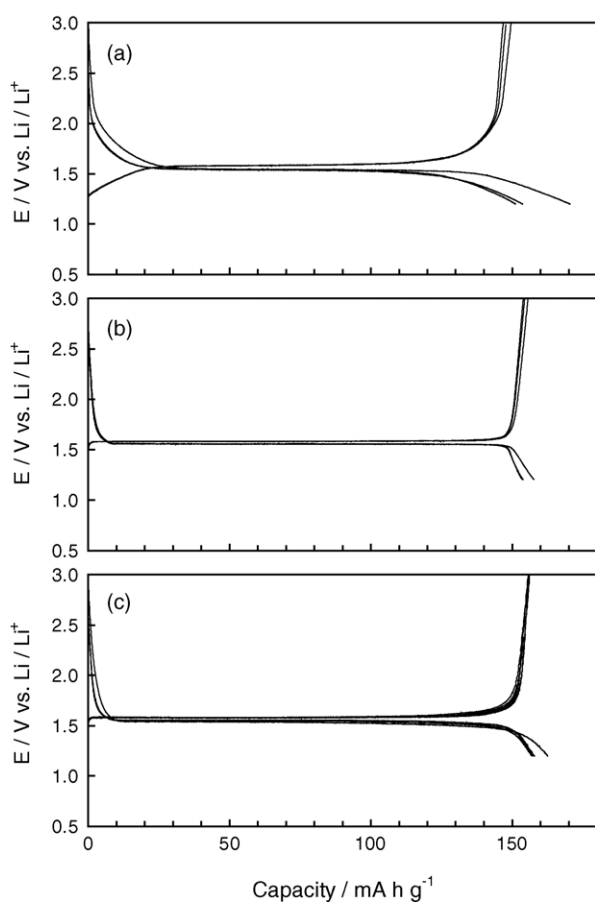


Fig. 4. Charge and discharge curves of  $\text{Li}_4\text{Ti}_5\text{O}_{12}$  samples in  $1\text{ mol dm}^{-3}$   $\text{LiClO}_4/\text{EC} + \text{DEC}$  (1:1 in volume) at 0.1 C rate.  $\text{Li}_4\text{Ti}_5\text{O}_{12}$  samples were heat-treated at  $500^\circ\text{C}$  for 3 h (a),  $800^\circ\text{C}$  in an electric furnace for 10 h (b), and  $800^\circ\text{C}$  in an infrared furnace for 1 min (c).

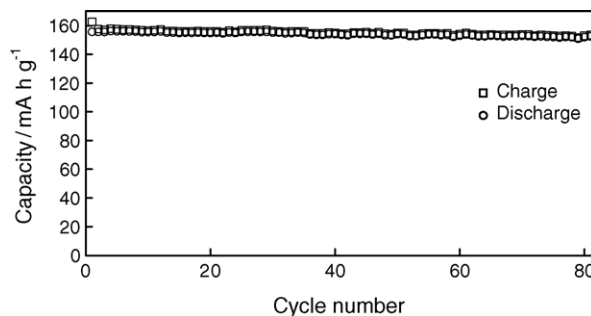


Fig. 5. Capacity changes of  $\text{Li}_4\text{Ti}_5\text{O}_{12}$  heat-treated at  $800^\circ\text{C}$  in an infrared furnace. Charge–discharge cycle test was carried out at 0.1 C rate.

of 1.50–1.20 V was considered due to  $\text{Li}^+$  ion insertion into the glassy part, while the plateau at 1.55 V was attributed to  $\text{Li}^+$  ion insertion into the crystallite. However, further investigations are needed to determine the mechanism of  $\text{Li}^+$  insertion into glassy lithium titanium oxide, which will be future work.

Fig. 5 shows charge–discharge cycle stability of the  $\text{Li}_4\text{Ti}_5\text{O}_{12}$  heat-treated at  $800^\circ\text{C}$  in infrared furnace. The  $\text{Li}_4\text{Ti}_5\text{O}_{12}$  showed a discharge capacity of  $160\text{ mA h g}^{-1}$  even at 80th cycle, and almost no degradation of the electrode by the repetition of charge and discharge was observed. This suggests the stable operation of the  $\text{Li}_4\text{Ti}_5\text{O}_{12}$  electrode as an anode for rechargeable lithium batteries.

#### 4. Conclusion

The spherical  $\text{Li}_4\text{Ti}_5\text{O}_{12}$  particles were prepared via an emulsion-gel process. The synthesis conditions for spherical  $\text{Li}_4\text{Ti}_5\text{O}_{12}$  such as the concentration of starting materials and heat treatment were optimized. The control on the concentration of TTIP was very important to obtain  $\text{Li}-\text{Ti}-\text{O}$  particles with narrow size distribution. It was found that the short heat treatment in an infrared furnace was useful to crystallize amorphous metal oxide powders without aggregation of particles or morphology change. The particle size of  $\text{Li}_4\text{Ti}_5\text{O}_{12}$  prepared under optimized condition was  $0.45\ \mu\text{m}$ . The obtained  $\text{Li}_4\text{Ti}_5\text{O}_{12}$  had a spinel-related

structure, and no impurity phase was detected. The prepared  $\text{Li}_4\text{Ti}_5\text{O}_{12}$  exhibited a discharge capacity of  $160 \text{ mA h g}^{-1}$ , and the charge–discharge cycle stability was excellent.

## References

1. Tarascon, J. M. and Armand, M., Issues and challenges facing rechargeable lithium batteries. *Nature*, 2001, **414**, 359–367.
2. Hasegawa, K. and Arakawa, Y., Safety study of electrolyte solutions for lithium batteries by accelerating-rate calorimetry. *J. Power Sources*, 1993, **43–44**, 523–529.
3. Dahn, J. R., Fuller, E. W., Obrovac, M. and von Sacken, U., Thermal stability of  $\text{Li}_x\text{CoO}_2$ ,  $\text{Li}_x\text{NiO}_2$  and  $\lambda\text{-MnO}_2$  and consequences for the safety of Li-ion cells. *Solid State Ionics*, 1994, **69**, 265–270.
4. Croce, F., Appetecchi, G. B., Persi, L. and Scrosati, B., Nanocomposite polymer electrolytes for lithium batteries. *Nature*, 1998, **394**, 456–458.
5. Thackeray, M. M., Manganese oxide for lithium batteries. *Prog. Solid State Chem.*, 1997, **25**, 1–71.
6. Ferg, E., Gummow, R. J., de Kock, A. and Thackeray, M. M., Spinel anodes for lithium-ion batteries. *J. Electrochem. Soc.*, 1994, **141**, L147–L150.
7. Ohzuku, T., Ueda, A. and Yamamoto, N., Zero-strain insertion material of  $\text{Li}[\text{Li}_{1/3}\text{Ti}_{5/3}]\text{O}_4$  for rechargeable lithium cells. *J. Electrochem. Soc.*, 1995, **142**, 1431–1435.
8. Scharner, S., Weppner, W. and Schmid-Beurmann, P., Evidence of two-phase formation upon lithium insertion into the  $\text{Li}_{1.33}\text{Ti}_{1.67}\text{O}_4$  spinel. *J. Electrochem. Soc.*, 1999, **146**, 857–861.
9. Kanamura, K., Naito, H. and Takehara, Z., Novel spinel oxides  $\text{Li}_{4/3}\text{Ti}_{5/3}\text{O}_4$  as electrochemical insertion materials for rechargeable lithium batteries. *Chem. Lett.*, 1997, 45–46.
10. Kanamura, K., Umegaki, T., Naito, H., Takehara, Z. and Yao, T., Structural and electrochemical characteristics of  $\text{Li}_{4/3}\text{Ti}_{5/3}\text{O}_4$  as an anode material for rechargeable lithium batteries. *J. Appl. Electrochem.*, 2001, **31**, 73–78.
11. Rho, Y. H. and Kanamura, K., Preparation of  $\text{Li}_{4/3}\text{Ti}_{5/3}\text{O}_4$  thin film electrodes by a PVP sol–gel coating method and their electrochemical properties. *J. Electrochem. Soc.*, 2004, **151**, A106–A110.
12. Zaghbi, K., Armand, M. and Gauthier, M., Electrochemistry of anodes in solid-state Li-ion polymer batteries. *J. Electrochem. Soc.*, 1998, **145**, 3135–3140.
13. Peramunage, D. and Abraham, K. M., Preparation of micron-sized  $\text{Li}_4\text{Ti}_5\text{O}_{12}$  and its electrochemistry in polyacrylonitrile electrolyte-based lithium cells. *J. Electrochem. Soc.*, 1998, **145**, 2609–2615.
14. Peramunage, D. and Abraham, K. M., The  $\text{Li}_4\text{Ti}_5\text{O}_{12}$ //PAN Electrolyte// $\text{LiMn}_2\text{O}_4$  rechargeable battery with passivation-free electrodes. *J. Electrochem. Soc.*, 1998, **145**, 2615–2622.
15. Ohzuku, T., Ariyoshi, K., Yamamoto, S. and Makimura, Y., A 3-Volt lithium-ion cell with  $\text{Li}[\text{Ni}_{1/2}\text{Mn}_{3/2}]\text{O}_4$  and  $\text{Li}[\text{Li}_{1/3}\text{Ti}_{5/3}]\text{O}_4$ : a method to prepare stable positive-electrode material of highly crystallized  $\text{Li}[\text{Ni}_{1/2}\text{Mn}_{3/2}]\text{O}_4$ . *Chem. Lett.*, 2001, 1270–1271.
16. Osseo-Asare, K. and Arriagada, F. J., Preparation of  $\text{SiO}_2$  nanoparticles in a non-ionic reverse micellar system. *Colloids Surf.*, 1990, **50**, 321–339.
17. Arriagada, F. J. and Osseo-Asare, K., Phase and dispersion stability effects in the synthesis of silica nanoparticles in a non-ionic reverse microemulsion. *Colloids Surf.*, 1992, **69**, 105–115.
18. Lindberg, R., Sjoblom, J. and Sundholm, G., Preparation of silica particles utilizing the sol-gel and the emulsion-gel processes. *Colloids Surf. A: Physicochem. Eng. Aspects*, 1995, **99**, 79–88.
19. Suda, S., Yoshida, T., Kanamura, K. and Umegaki, T., Formation mechanism of amorphous  $\text{Na}_2\text{O-SiO}_2$  spheres prepared by sol–gel and ion-exchange method. *J. Non-Cryst. Solids*, 2003, **321**, 3–9.